Journal of Molecular Liquids 411 (2024) 125799

Contents lists available at ScienceDirect

Journal of Molecular Liquids

journal homepage: www.elsevier.com/locate/molliq

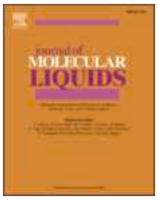

Experimental investigation and molecular dynamics study on the influence of non-ionic fluorocarbon solutions on the fast-wetting mechanism of coal dust

Kai Wang, Min Xu, Biao Zhou *, Dezheng Wang, Kaijie Chen

School of Emergency Management and Safety Engineering, China University of Mining & Technology (Beijing), Beijing 100083, China
State Key Laboratory Coal Resources and Safe Mining, Beijing 100083, China
Beijing Key Laboratory for Precise Mining of Intergrown Energy and Resources, China University of Mining and Technology (Beijing), Beijing 100083, China

ARTICLE INFO

Keywords:
Molecular structure
Adsorption energy
MD simulation
Hydrogen bond
Fluorocarbon structure

ABSTRACT

To explore methods for enhancing the wetting performance of coal dust to mitigate its hazards, this study selected four different structures of non-ionic fluorocarbon solutions: perfluorinated propyl acrylate (PFPA), perfluorooctyl acrylate (PFTA), perfluorooctyl sulfonyl phenyloxy ethyl methylacrylate (PPM), and perfluoro propanoic acid (PFA). The dynamic wetting performance and mechanisms of these solutions on coal dust were measured and analyzed through kinetic calculations. The results indicate that all four fluorocarbon solutions achieve optimal wetting performance at a concentration of 0.3 %. Comprehensive analysis shows that their wetting ability follows the order PFPA > PFTA > PPM > PFA. Further analysis reveals that coal dust treated with PFPA shows an increase in structures such as —COOH and C—O. The relative concentration distribution indicates partial overlap between the fluorocarbon solution and water, with an overlap range of 8.2 Å. Additionally, the maximum diffusion coefficient is 0.577 Å/ps, and the system's adsorption energy is the highest at −5757.25 kcal/mol.

1. Introduction

Coal resources play a crucial role in global energy supply [1–5]. With the continuous improvement of mechanized mining equipment in underground coal mines, the amount of coal mining is also increasing [6,7]. Without any dust prevention measures, coal dust in mine could exceed the coal dust standard stipulated by the state [8–10]. At present, spray dust reduction, personal protection, ventilation and dust removal are usually used to prevent coal dust disasters underground [11,12]. Wet spray dedusting is widely used underground because of its simple operation and low cost. The wet spray dedusting solution is based on water. However, due to the high surface tension of water, it is not enough to wet the coal dust, and the ideal wetting effect cannot be achieved, resulting in low dust removal efficiency [13,14]. Therefore, the right amount of wetting agent is usually added to the water to improve the wettability of the water, enhance the efficiency of dust reduction in the well, and improve workplace safety. The dust suppressant can reduce water's surface tension, so water can more easily spread on the surface and penetrate small spaces [15,16]. When added to water, dust suppressants make it easier for water to wet coal dust particles, causing them to clump together and settle out of the air. It helps prevent dust from becoming airborne and reduces the risk of respiratory illness or explosion [17]. Some common wetting agents used for coal dust control include non-ionic surfactants, anionic surfactants and cationic surfactants [18].

Currently, considerable research is analyzing the interaction between the surface structure of coal and surfactants from a microscopic perspective [19–21]. Studies have revealed that changes in the relative content of functional groups on coal samples can directly reflect the quantitative relationship between surfactants and their wetting properties [22–24]. Coal, as a carbonaceous mixture consisting of various functional group structures [25,26], is composed of major organic compounds such as alkanes, fatty acids, phenols, aldehydes, ketones, cycloalkanones, aromatic compounds, and heterocyclic compounds, interconnected through aromatic ring systems, side chain structures, and itching functional groups [27–29]. The higher the degree of coalification of coal samples, the more complex their composition becomes [30]. These organic compounds can adsorb onto the surface of coal dust, affecting the interfacial activity of coal dust and slowing down the wetting process between coal dust and dust suppression solutions [31].

---

* Corresponding author at: Room 226, No. 11, Xueyuan Road, Haidian District, Beijing 100083, China.

https://doi.org/10.1016/j.molliq.2024.125799
Received 19 March 2024; Received in revised form 14 August 2024; Accepted 15 August 2024

Table 1
Industrial and elemental analysis of coal samples.

Industrial					Elemental				
Mad/%	Ad/%	Vd/%	FCdaf/%	–	Cdaf/%	Hdaf/%	Odaf/%	Ndaf/%	Sdaf/%
7.05	8.46	27.68	56.59		81.11	4.52	11.26	1.09	0.34

Compared to traditional surfactants, fluorocarbon solutions exhibit high surface activity and excellent wetting properties [32,33]. Fluorocarbon solution molecules form hydrophobic and hydrophilic layers in water; the fluorine-containing hydrophobic layer faces the water, while the hydrophilic layer faces the coal dust surface. Functional groups on the coal dust surface can interact with the polar functional groups in fluorocarbon solutions, forming a dense adsorption layer that reduces the surface energy of the coal dust and achieves wetting. Due to their high thermal stability, fluorocarbon solutions maintain their performance under high temperatures, ensuring long-term effective wetting. Dai examines the adsorption kinetics of non-ionic fluorochemical surfactants (4-hydroxyethyl ether) (perfluoroalkyl) in coalbed methane and finds that the adsorption process of fluorochemical solutions on the coal surface is spontaneous and endothermic [34]. Niu investigates the wetting properties of fluorochemical surfactants (OBS) on coal dust. The surface tension of 0.06 % OBS is reduced to 17.6 mN/m, with a median particle size of coal dust reaching 60.25 μm after wetting [35]. These findings indicate the significant role of fluorochemical materials in dust suppression, effectively preventing dust hazards.

Previous studies have used various molecular dynamics (MD) simulation software to analyze the wetting and adsorption mechanisms between solutions and coal dust at the molecular level [36–39]. MD simulations, which simulate the evolution of atoms or molecules over time by numerically solving Newton's equations of motion [40–42]. MD simulations provide systematic dynamic information to study material properties, molecular structures, and chemical reaction dynamics [43–48]. Gan et al. established a model of a water-surfactant-low-rank coal system. The simulation results demonstrated the strong adsorption capability of dodecyl ether ammonium sulfate, partly attributed to the hydrolyzed cation and EO groups. However, the article had some limitations [49]. Wang et al. utilized MD simulations to reveal the fixation mechanism of a novel dust fixative (GC-TG-JFC) on coal dust [50]. Zhao et al. investigated the impact mechanism of SiO_2-H_2O nanofluid on the wetting behavior of low-rank coal dust using MD simulations [51]. Wang explored the influence and action mechanism of inhibitors on the molecular structure of coal using MD simulation methods, demonstrating that inhibitors can significantly alter the molecular structural characteristics of coal and inhibit its low-temperature oxidation process [52].

To comprehensively understand the impact of different fluorocarbon structures on coal dust wettability, we selected four non-ionic fluorocarbon solutions with different oxygen-containing functional groups, aromatic hydrocarbons, and fluorocarbon chain lengths (PFPA, FTA, PPM, PFA) for experimentation. This study aims to improve the screening efficiency of wetting agents by identifying fluorocarbon structures that achieve rapid wetting at minimal dosages. We conducted various static and dynamic wetting experiments and MD simulations on four fluorocarbon solutions with similar structures but different properties. First, we performed surface tension experiments to select the optimal wetting properties of the four fluorocarbon solutions and analyzed the surface characteristics and adsorption properties of coal dust after treatment using Fourier-transform infrared spectroscopy (FTIR). Contact angle experiments, reverse capillary imbibition experiments, and Walker sedimentation experiments were used to test and analyze the differences in performance during different wetting processes: collisional wetting, adsorption wetting, and immersion wetting. Finally, we revealed the effects of different fluorocarbon solution structures on coal dust wettability at the molecular levels by analyzing the equilibrium conformations, relative concentration distributions, mean square displacements (MSD), diffusion coefficients, and radial distribution functions of different systems.

Table 2
Introduction to the fluorocarbon solutions used in the experiment.

Experimental reagents	Active component	Molecular formula	Type
Perfluoro propyl Acrylate	24–26 %	$CH_2 = CHC(O)OC_3F_7$	Non-ionic
Perfluorooctyl Acrylate	24–26 %	$CH_2 = CHC(O)OC_8F_{17}$	Non-ionic
Perfluorooctyl sulfonyl Phenoxy ethyl Methacrylate	24–26 %	$C_8F_{17}SO_2OC_6H_4OH$	Non-ionic
Perfluoro propanoic Acid	26–28 %	CF_3CF_2COOH	Non-ionic

2. Wetting testing experiments and MD simulations

2.1. Selection and preparation of coal samples and solutions

Samples are carefully selected from the Red Qinghe coal mine in Inner Mongolia, China. These coal samples undergo stripping, crushing, and sieving for preparation. Subsequently, 5 g of coal particles are taken, washed several times with distilled water, and dried at temperatures not exceeding 80 °C. After grinding, the samples are sieved through a 300-mesh standard sieve for experiment use. Industrial and elemental analyses of the coal samples follow the national standard of China, "Methods for Industrial Analysis of Coal" (GB/T 212-2008), determining the mass fractions of fixed carbon, ash, volatile matter, moisture, and significant elements in the coal samples, as shown in Table 1.

Different types and masses of fluorocarbon solution reagents PFPA, PFTA, PPM, and PFA are weighed using a balance scale. Simultaneously, distilled water solute is measured using a graduated cylinder. Subsequently, the solutions are mixed to prepare fluorocarbon solutions of varying concentrations (0.01 %, 0.05 %, 0.07 %, 0.1 %, 0.2 %, 0.3 %) for

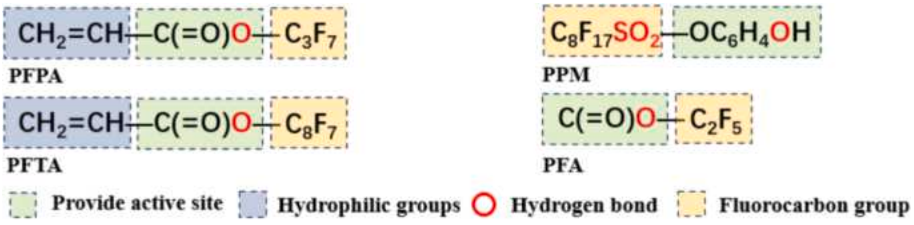

Fig. 1. The molecular structures of the four fluorocarbons.

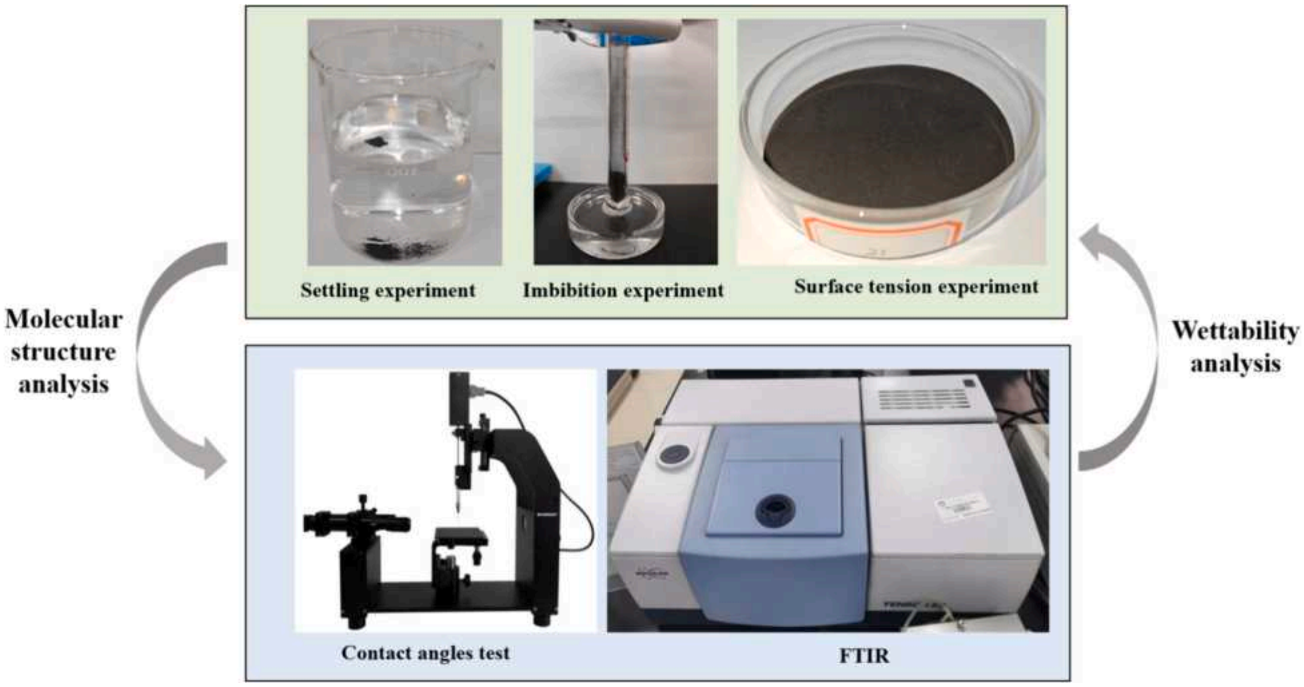

Fig. 2. The experimental procedure.

experimentation. Fig. 1 illustrates the molecular structures of the four different fluorocarbon solutions. Table 2 lists the primary reagents and molecular formulas used in the experimental procedure.

2.2. *Wettability testing experiment*

2.2.1. *Contact angle measurement experiment*

The contact angle is the most direct parameter reflecting wetting strength. When a water droplet contacts coal dust, a contact angle forms, indicating the degree of wetting. At equilibrium, the angle between the solid and liquid is the contact angle, denoted by θ. Cylindrical coal pieces (1 mm thick and 1 cm in diameter) are prepared using a benchtop briquette press at 20 MPa. The contact angle between distilled water and coal dust is measured using an optical droplet shape analyzer (model JC2000DM). To ensure accuracy, the data are averaged over three measurements. The contact angle between coal dust and deionized water is 79.47°.

2.2.2. *Imbibition experiment*

The prepared coal powder is dried at 100 ± 5 °C for 2 h and, after cooling, stored in a sealed bag. A glass tube with a 15 mm diameter open end is sealed with filter paper and filled with about 5 g of coal powder. The tube is vibrated for 10 min to form a dense column, then vertically fixed with its bottom immersed in a glass dish. The experimental solution is added to the dish until it contacts the tube's bottom. Timing starts at this point, recording the time for water to infiltrate to different heights. The experiment ends when the infiltration height stabilizes. Each group repeats the experiment three times to minimize errors.

2.2.3. *Settling experiment*

The settling experiment provides a more intuitive assessment of the wetting performance of coal dust [53]. When coal dust contacts the

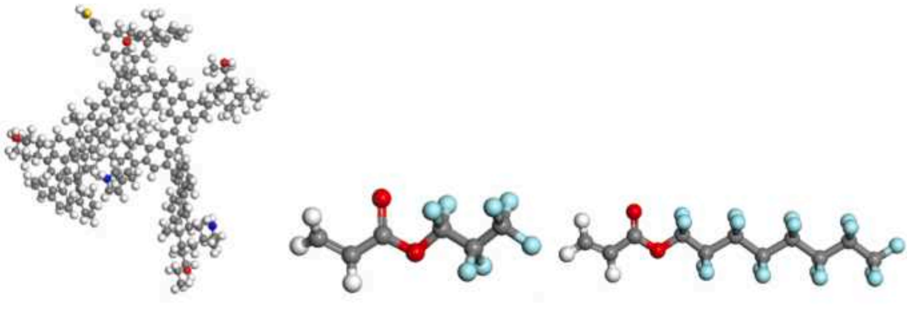

(a) Coal (b) PFPA (c) PFTA

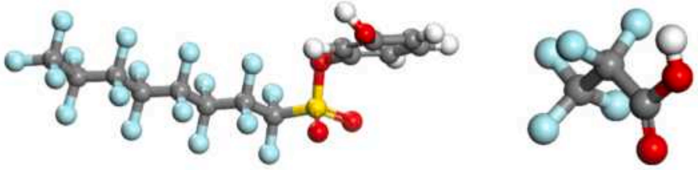

(d) PPM (e) PFA

Fig. 3. Molecular models of coal and four types of fluorocarbon solutions.

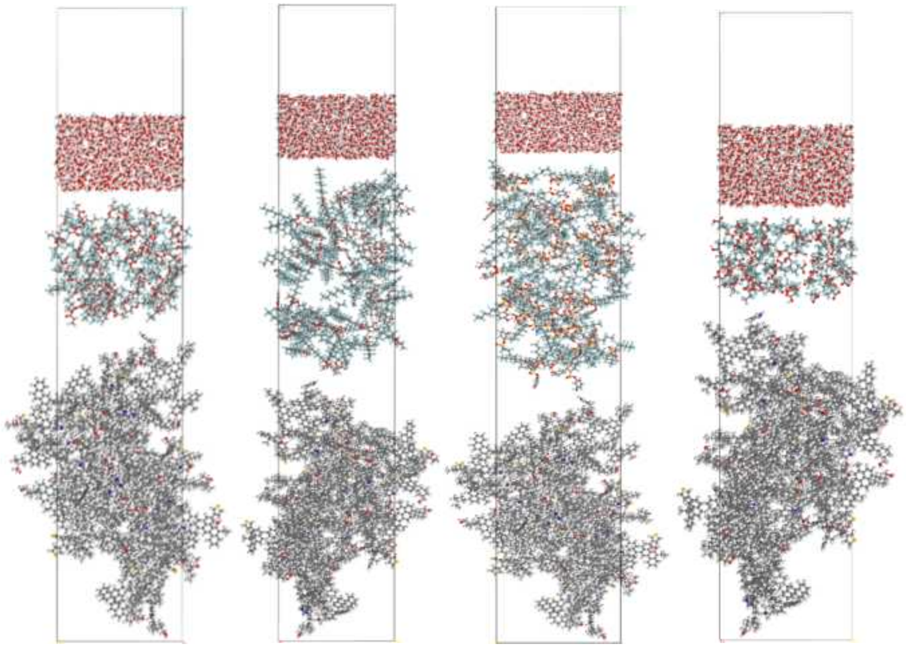

(a) System 1 (b) System 2 (c) System 3 (4) System 4

Fig. 4. Four different simulation systems.

solution, it absorbs water and settles; a faster settling rate indicates better water absorption and superior wetting performance. This method is easy to operate and effective, making it a common choice for determining coal dust wetting properties. The following is a specific flow figure of the experiment, seen in Fig. 2.

2.3. *FTIR experiment*

This experiment utilizes FTIR to measure changes in the functional group structures of coal samples after interaction with various fluorocarbon solutions. The coal samples are uniformly mixed with KBr at a ratio of 1:100 and further homogenized by grinding in an agate mortar. The resulting powder is then formed into transparent pellets and placed in the infrared spectrometer. The influence of different concentrations and types of fluorocarbon solutions on the functional groups of coal samples is assessed by analyzing the absorption spectra's shape, intensity, and peak area.

2.4. *MD simulation*

As shown in Fig. 3, the molecular formula of bituminous coal is $C_{42}H_{44}O_4N_2S$, featuring essential structural components such as carboxyl groups, benzene rings, aromatic hydrocarbons, ketone groups, phenol groups, and alcohol groups. Three-dimensional models are established, incorporating coal molecules, fluorocarbon solution molecules, and water molecules. Following geometric optimization and annealing calculations, the molecular models of PFPA, PFTA, PPM, and PFA are shown in Fig. 3. Simulations are conducted using Materials Studio 2020. Using the amorphous cell module and the Build Layer tool, four simulation systems are set up: PFPA/coal/H_2O (System 1), PFTA/coal/H_2O (System 2), PPM/coal/H_2O (System 3), and PFA/coal/H_2O (System 4). Each system comprises 20 coal molecules, 100 fluorocarbon molecules, and 1000 water molecules, as shown in Fig. 4. MD simulations are performed using the COMPASS III force field in the Forcite module.

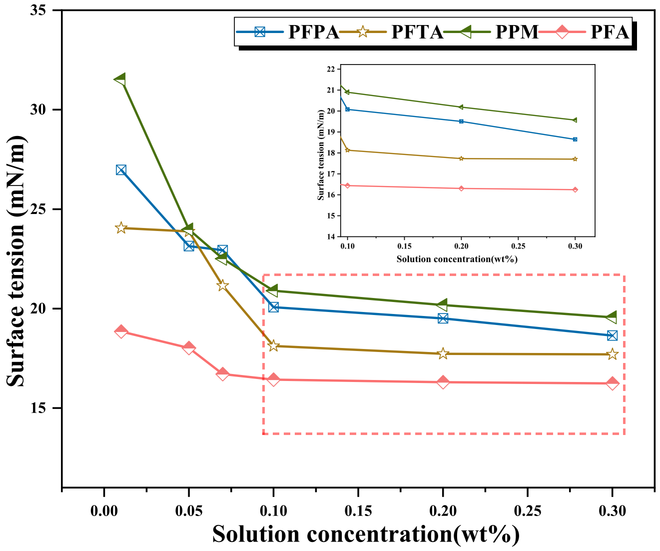

Fig. 5. The surface tension of the four fluorocarbon solutions at different concentrations.

3. Results and discussion

3.1. *Analysis of experimental results*

3.1.1. *Analysis of wetting preference experiment*

The variation of surface tension of fluorocarbon solutions reflects their adsorption status at the gas–liquid interface. It is also crucial in reflecting coal dust's wetting effectiveness and dust reduction efficiency. Therefore, surface tension tests were conducted on the four fluorocarbon solutions at different concentrations. As shown in Fig. 5, with the increase in fluorocarbon solution concentration, the surface tension of all four solutions gradually decreases. The increase in fluorocarbon solution concentration can enhance the interactions between fluorocarbon solution molecules, leading to their aggregation at the solution surface to

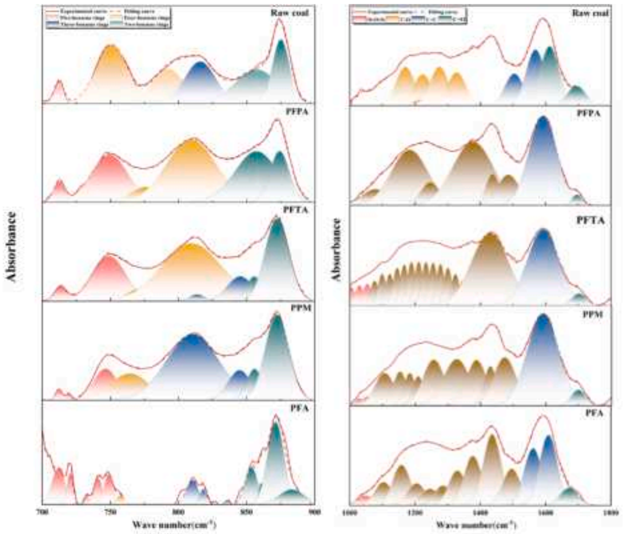

(a) The aromatic hydrocarbon structures (b) The oxygen-containing functional groups

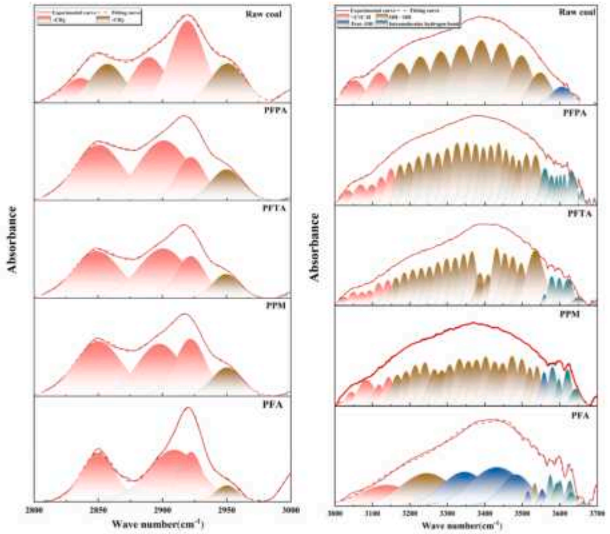

(c) The aliphatic hydrocarbon structures (d) The hydrogen bond structures

Fig. 6. Fitting peaks of different absorption functional groups.

form a stable fluorocarbon surface layer. This surface layer can reduce the interactions between molecules and water and between fluorocarbon chains, gradually decreasing the surface tension and stabilizing upon reaching the critical micelle concentration.

The different molecular structures of the four non-ionic fluorocarbon solutions result in their distinct properties, primarily manifested at the same concentration level (concentration $>$0.1 %). The surface tension of the solutions follows the order of PFA $>$ PFTA $>$ PFPA $>$ PPM, indicating that PFA exhibits the most potent ability to reduce surface tension, while PPM exhibits the weakest. Notably, the difference in molecular structure between PFPA and PFTA lies in the length of the fluorocarbon chain, leading to variations in surface tension with increasing concentration. The fluorocarbon chain in PFPA is shorter than that in PFTA, and the length of the perfluoroalkyl chain directly affects the surface tension. Generally, longer fluorocarbon chains can form a more uniform and effective surface layer to reduce surface tension because they create a surface layer in water that is more resistant to penetration by water molecules. Longer fluorocarbon chains may be more likely to form ordered arrangements at the molecular level, resulting in a more orderly and denser surface layer. This ordered arrangement contributes to better surface coverage and lower surface tension. PFPA, due to its shorter fluorocarbon chains, may exhibit a relatively loose arrangement at the molecular level, resulting in a less uniform surface layer and higher surface tension. The above indicates that the structural differences in surfactant molecules significantly influence their adsorption configuration at the gas–liquid interface.

3.1.2. Analysis of wetting structure

Previous studies indicate that different surfactant solutions can improve the wetting properties of coal dust by altering its surface structure. The adsorption status of surfactants on mineral particle surfaces can be analyzed by comparing the infrared spectra of mineral particles before and after surfactant adsorption. The original infrared spectral data are fitted using ONMIC software to obtain peak fitting and peak areas. The fitted peak results of coal samples treated with PFPA, PFTA, PPM, and PFA are presented in Fig. 6.

Based on the classification of functional groups in coal, the entire spectrum is divided into four parts: the absorption region of aromatic hydrocarbon structures (700–900 cm^{-1}), the absorption region of oxygen-containing functional groups (1000–1800 cm^{-1}), the absorption

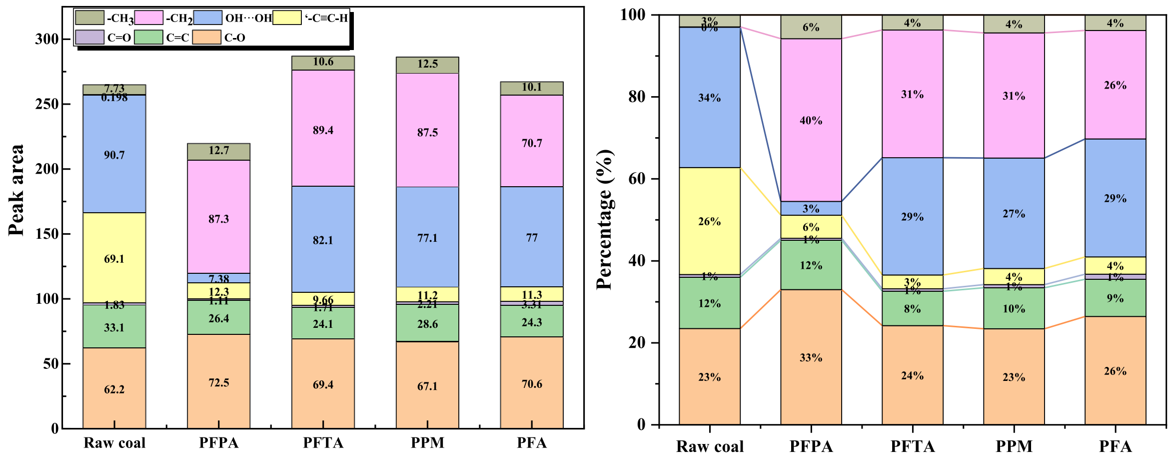

(a) Changes in the area of absorption peaks (b) Percentage changes in the area of absorption peaks

Fig. 7. Main functional group content change.

region of aliphatic hydrocarbon structures (2800–3000 cm^{-1}), and the absorption region of hydrogen bond structures (3000–3600 cm^{-1}). Compared to the raw coal, different fluorocarbon solutions exhibit variations in characteristic absorption peaks of the coal samples, primarily within the range of oxygen-containing functional groups and hydrogen bond structures. Coal, as a compound with a complex chemical structure composed of multiple functional groups, contains many aromatic and aliphatic hydrocarbon structures, resulting in its hydrophobic solid surface structure. In the absorption regions of aromatic hydrocarbon structures and hydrogen bond structures, it is evident that PFA exhibits fewer fitted absorption peaks than the raw coal and coal samples treated with other fluorocarbon solutions. Conversely, in the absorption region of oxygen-containing functional group structures, a reduction in the number of absorption peaks corresponding to the C═O structure is observed in coal samples treated with different fluorocarbon solutions, especially in those treated with PFTA, PPM, and PFA, where Si—O—Si absorption peaks appear.

For the same wavelength range under identical testing conditions, the changes in the absorption peaks of coal functional groups affected by fluorocarbon solutions can be semi-quantitatively expressed using peak areas and their percentages, as shown in Fig. 7 (a) and (b). Compared to raw coal, the most significant changes observed in coal samples treated with PFPA, PFTA, PPM, and PFA are the increase in $—CH_2$ content and the decrease in —C≡C—H content, with corresponding area percentages of 87.3 and 12.3, 89.4 and 9.66, 87.5 and 11.2, and 70.5 and 11.3, respectively. These results indicate that the different lengths of perfluoroalkyl chains in the two fluorocarbon molecules may lead to different interactions with the coal surface, resulting in distinct absorption peaks. The increase in $—CH_2$ content is attributed to the interaction between introduced fluorocarbon molecules and the coal surface during treatment, leading to an increase in $—CH_2$ functional groups. The perfluoroalkyl chains can cover and interact, making the coal surface more hydrophobic, thus increasing the $—CH_2$ content. The decrease in —C≡C—H content is due to the introduction of fluorocarbon molecules during the wetting process of coal dust, where the introduced fluorocarbon molecules may react with or competitively adsorb to the functional groups containing C≡C—H bonds on the coal surface, resulting in a decrease in C≡C—H content. The introduction of fluorocarbon chains may alter the electronic environment of the coal surface, affecting the adsorption of functional groups containing —C≡C bonds.

Compared to the original coal sample, the proportion of $—CH_2$ in coal samples treated with PFPA and PFTA solutions increases from 0.12 % to 40 % and 31 %, respectively, while OH…OH decreases from 34 % to 3 % and 29 %, and C—O increases from 23 % to 33 % and 24 %. A denser arrangement of fluorocarbon chains on the surface of coal samples treated with PFPA and PFTA solutions facilitates the formation of a uniformly distributed fluorocarbon layer, increasing the proportion of $—CH_2$. The perfluoropropyl acrylate functional group in PFPA solution may interact with hydroxyl groups on the coal surface, decreasing the proportion of OH…OH. Conversely, the perfluorooctyl acrylate functional group in PFTA may interact less with hydroxyl groups on the coal surface, increasing the proportion of OH…OH. PFPA contains hydrogen-containing functional groups, which may interact with the C—O functional groups on the coal surface, increasing the proportion of C—O. The interaction between hydrogen-containing and C—O functional groups may be relatively strong. The perfluorooctyl acrylate functional group in PFTA may interact less with C—O functional groups on the coal surface, resulting in a relatively lower proportion of C—O. The longer perfluoroalkyl chain may limit the interaction with C—O functional groups.

The differential impact of PPM and PFA solutions on the functional groups of coal samples is similar to the changes observed in coal samples

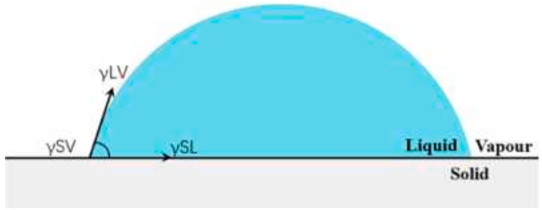

(a) Diagram of solid/liquid/gas three-phase interaction

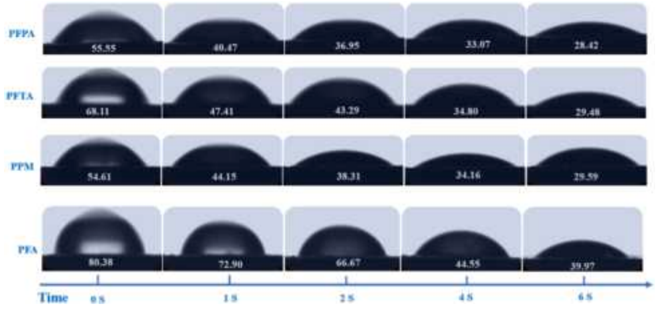

(b) The contact angles between fluorocarbon solutions and coal

Fig. 8. The contact angles.

treated with PFTA solution. Solutions containing the same fluorocarbon chain length, such as PFTA and PPM, exhibit similar alterations in functional group structures. Compared to the original coal sample, the content of —CH_2 structures on the surface of coal samples treated with the four fluorocarbon solutions decreases. In contrast, the content of C≡C—H structures decreases. Therefore, treating the functional group structure on the coal surface can significantly enhance its wetting performance.

3.1.3. Analysis of collisional contact wetting performance

The wetting process between fluorocarbon solutions and coal particles involves a series of steps, including collision, contact, and spreading between the liquid substance and the solid surface, forming a solid/liquid contact interface. These steps comprise collisional wetting, adsorptive wetting, and immersion wetting. In Fig. 8(a), the tensions between the solution and air, the solution and coal sample, and the coal sample and air are represented respectively by γLV, γSL, and γSV. At equilibrium, the relationship between the tensions among the three phases and the equilibrium contact angle θ can be expressed using Young's Equation [54].

$$\gamma LV \cdot \cos\theta = \gamma SV - \gamma SL \tag{1}$$

Theoretically, the decrease in γLV implies a weakened attraction between the internal atoms of the liquid and the surface atoms, making it easier for the liquid to overcome gravity, leading to surface expansion and facilitated spreading. A reduction in γSL indicates an increased attraction between the solid and liquid atoms, causing the inner atoms of the liquid to be drawn towards the solid–liquid interface, thus promoting spreading. Hydrophobic tail chains of surfactant molecules begin to adsorb on the coal surface, initiating the adsorptive wetting. This stage involves the migration of surfactant molecules from the liquid solution to the solid coal surface, where initial adsorption establishes a preliminary adhesion between the surfactant and the coal surface. Subsequently, the coal particles are gradually enveloped and covered by a liquid film, resulting in diffusive wetting. During this process, the area of the solid/liquid and liquid/gas interfaces gradually increases while the area of the solid/gas interface diminishes. The hydrophobic portion of the coal surface undergoes modification, enhancing the contact area between the surfactant and the coal surface, thereby promoting further wetting. When the liquid film completely submerges and settles the coal particles, the system consists only of the solid/liquid interface. Surfactant molecules adsorb onto this interface, facilitating the continuous penetration of liquid molecules into the coal surface through hydrophilic interactions. In summary, the wetting process between fluorocarbon liquid solutions and coal particles still involves collisional wetting, adsorptive wetting, and immersion wetting. Subsequent wetting analysis can further investigate the kinetic characteristics, wetting performance, and interaction mechanisms between surfactants and coal particles during these wetting processes. It includes a quantitative study of the attachment, spreading, and impregnation effects of different surfactant solutions on wetting coal particles, providing insight into the mechanisms of action of surfactants in the wetting process described as immersion wetting, where the presence of surfactants facilitates the penetration of liquid molecules into the coal surface, enhancing wetting effectiveness.

The contact angle experiments are conducted on the 3 % concentration of the four fluorocarbon solutions, and the contact angles of each surfactant solution change over time, as shown in Fig. 6. The process of collision contact wetting covers the transition from non-contact to contact between the liquid and solid, thereby evolving the liquid–gas and solid–gas interfaces into the solid–liquid interface. In this process, the work done, *Wa*, can be represented using the contact angle and surface tension, as per Eq. (2), utilizing experimental data. The results of *Wa* for different fluorocarbon solutions are presented (PFPA = 43.46 mJ/m^2, PFTA = 32.88 mJ/m^2, PPM = 36.32 mJ/m^2, PFA = 28.68 mJ/m^2). It demonstrates a trend in *Wa*: PFPA > PPM > PFTA > PFA. The main reason for this difference is the slight variations in surface tension and final contact angle among the four fluorocarbon solutions at a 3 % concentration.

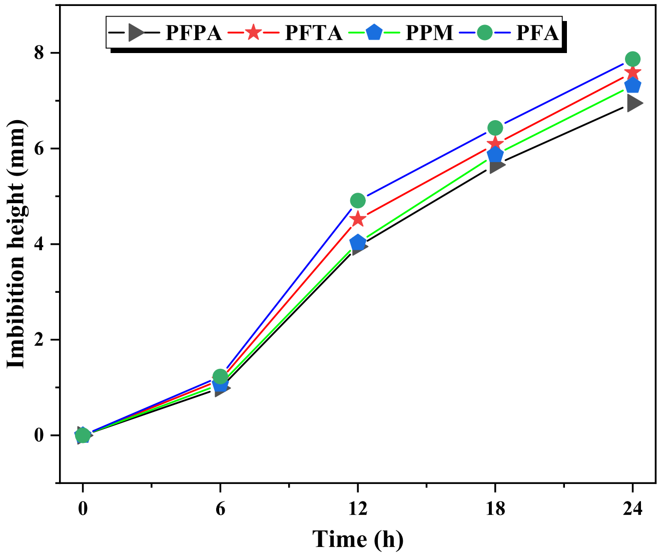

Fig. 9. The change in infiltration height over time varies.

$$Wa = \gamma SV + \gamma LV - \gamma SL = \gamma LV(\cos\theta + 1) \tag{2}$$

In the Equation, *Wa* represents the maximum work that the system can do externally during the collision contact wetting process, which is the minimum work required by the external environment to separate the solid and liquid from the solid–liquid interface. The more extensive *Wa*, the stronger the bonding between the solid–liquid interface. *Wa* can be used to characterize the bonding ability of the solid–liquid interface and the magnitude of the intermolecular interaction forces between the two phases.

However, for different types of surfactant solutions with the same concentration, if their surface tensions are slightly different, the change in dynamic contact angle should be considered to evaluate their wetting performance more comprehensively on coal dust. As shown in Fig. 8(b), the decreasing rates of contact angles for the four fluorocarbon solutions are in the following order: PFA > PFTA > PPM > PFPA. The comprehensive analysis above indicates significant differences in the results under different evaluation criteria, suggesting slight variations in the adhesion and wetting performance of the four fluorocarbon solutions on coal dust. Therefore, the wetting performance of these four surfactants cannot be accurately evaluated solely through single adhesion and diffusion wetting.

3.1.4. Analysis of adsorptive wetting performance

Fig. 9 shows that the osmotic heights of the four solutions within the first 6 h are relatively low, with PFA exhibiting the highest osmotic height at 1.23 mm. It is attributed to the superior fluidity of PFA compared to the other three medium solutions, allowing the hydrophilic functional groups to engage in osmosis. However, due to the higher

Table 3
Quality of each glass tube at different times.

Time (h)	Quality (mg)			
	PFPA	PFTA	PPM	PFA
0	0	0	0	0
6	29	29	30	29
12	72	79	78	82
18	101	129	107	134
24	139	158	148	162

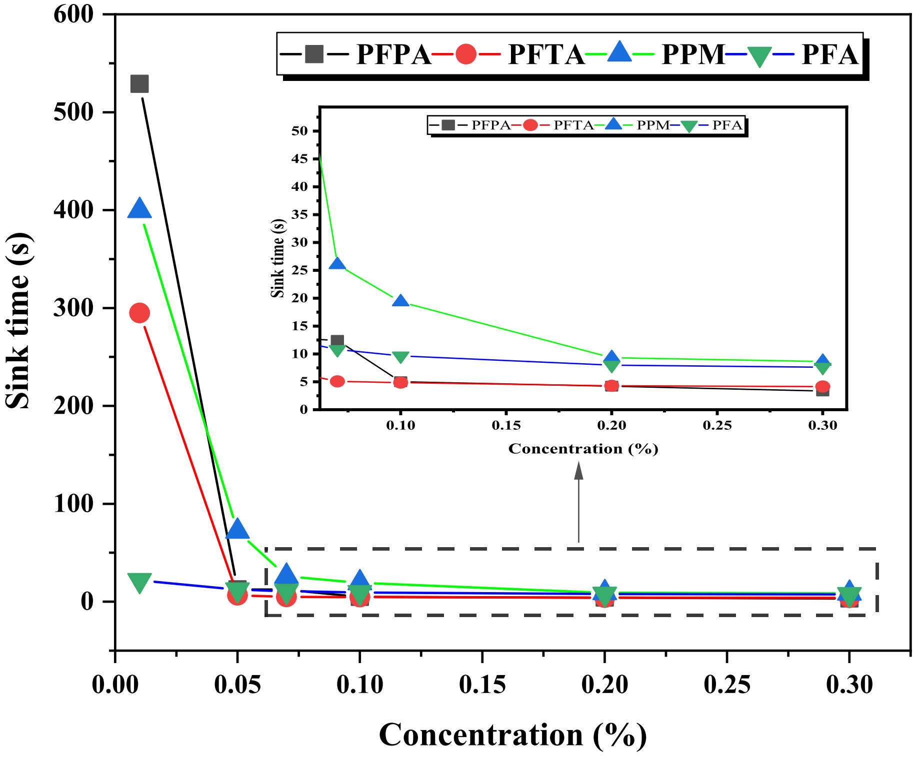

Fig. 10. The sink time of coal dust in the four fluorocarbon solutions.

viscosity and poorer fluidity of the other three solutions, their osmotic heights are lower than that of PFA. At 6 h, the osmotic heights of the four solutions are essentially the same. Over time, the osmotic heights of the four fluorocarbon solutions continue to increase, with PFA consistently higher than the other three solutions. At 24 h, the height sequence is as follows: PFA > PFTA > PPM > PFPA.

Table 3 shows that during the adsorption wetting and reverse osmosis absorption experiment, the coal powder inside the glass tubes absorbs the solution through capillary action, thereby increasing the total mass inside the glass tubes. The differences in mass among the four fluorocarbon solution-filled glass tubes are insignificant within the first 6 h. However, with increasing time, at 12 h and 24 h, the glass tube filled with PFPA shows the slightest increase in mass, while the mass increase in the glass tube filled with PFA remains consistently the highest. Combined with Fig. 10, the osmotic height of the glass tube filled with PFA is also higher than the other three solutions. At 24 h, the order of mass magnitude is as follows: glass tube filled with PFA > glass tube filled with PFTA > glass tube filled with PPM > glass tube filled with PFPA.

Furthermore, the relationship between the upward infiltration height of the solution inside the glass tube and the surface tension contact angle can be expressed by Eq. (3).

$$h = \frac{2\sigma\cos\theta}{\rho g r} \tag{3}$$

In the Equation, h represents the height, mm; ρ denotes the density of the solution, g/mL; g stands for the gravitational acceleration, N/kg; r signifies the inner radius of the glass tube, mm; σ represents the magnitude of the surface tension, mN/m; and θ indicates the size of the contact angle, °. This method can obtain the capillary forces of different fluorocarbon solutions (PFPA = 2.2453, PFTA = 11.379, PPM = 5.777, PFA = 14.623).

Theoretical calculations perfectly match experimental results, confirming the accuracy of their reverse osmotic height and osmotic mass ranking. Theoretical analysis of the reverse osmotic action of fluorocarbon solutions is conducted based on theoretical calculations and experimental results. In the experiment, when the glass tube contacts the solution, the capillary force generated by PFPA is weaker than the other three fluorocarbon solutions, leading to a weaker osmotic effect. The hydrophobic groups of PFA and PFTA attract coal dust. Simultaneously, under the influence of interaction forces, water molecules are attracted by the PFA and PFTA hydrophilic groups, scurrying towards the coal layer to permeate it, thereby quickly wetting it. As water molecules are drawn toward the coal dust, the hydroxyl groups (—OH) in the fluorocarbon solution also migrate toward the coal dust, creating a continuous traction effect facilitating the wetting of coal dust by the solution.

3.1.5. Analysis of immersion wetting performance

As shown in Fig. 10, when the solution concentration is below 0.05 %, the settling time of PFA is significantly shorter than that of PFPA, PFTA, and PPM, far less than 25 s, indicating that at low concentrations, PFA exhibits excellent immersion wetting performance. However, as the solution concentration exceeds 0.05 %, the settling time of PFTA surpasses that of the other three fluorocarbon solutions. With the increase in fluorocarbon solution concentration, the settling time of coal dust in the four solutions decreases first and then stabilizes. This phenomenon arises because when the solution concentration is below its critical micelle concentration, the surface tension of the solution significantly decreases, weakening the energy barrier at the interface and allowing coal dust to penetrate the interface into the solution quickly. When the concentration of the four solutions reaches 2 %, the settling time stabilizes, with both PFPA and PFTA settling in less than 5 mins. From this result, it can be inferred that at this concentration, the surface tension of PFTA also stabilizes.

Additionally, the increase in the content of —CH_2 and C—O structures in coal dust and the increase in adsorption density between coal dust particles enhance their ability to wet coal dust. It indicates that the wetting performance of fluorocarbon solutions is improved when the adsorption density on the coal dust surface increases. Although the surface tension of the PFA solution is relatively low, its wetting time is longer than that of the PFTA solution. This phenomenon may be due to the hydrophobic nature of the trailing fluorocarbon carbon chain of the

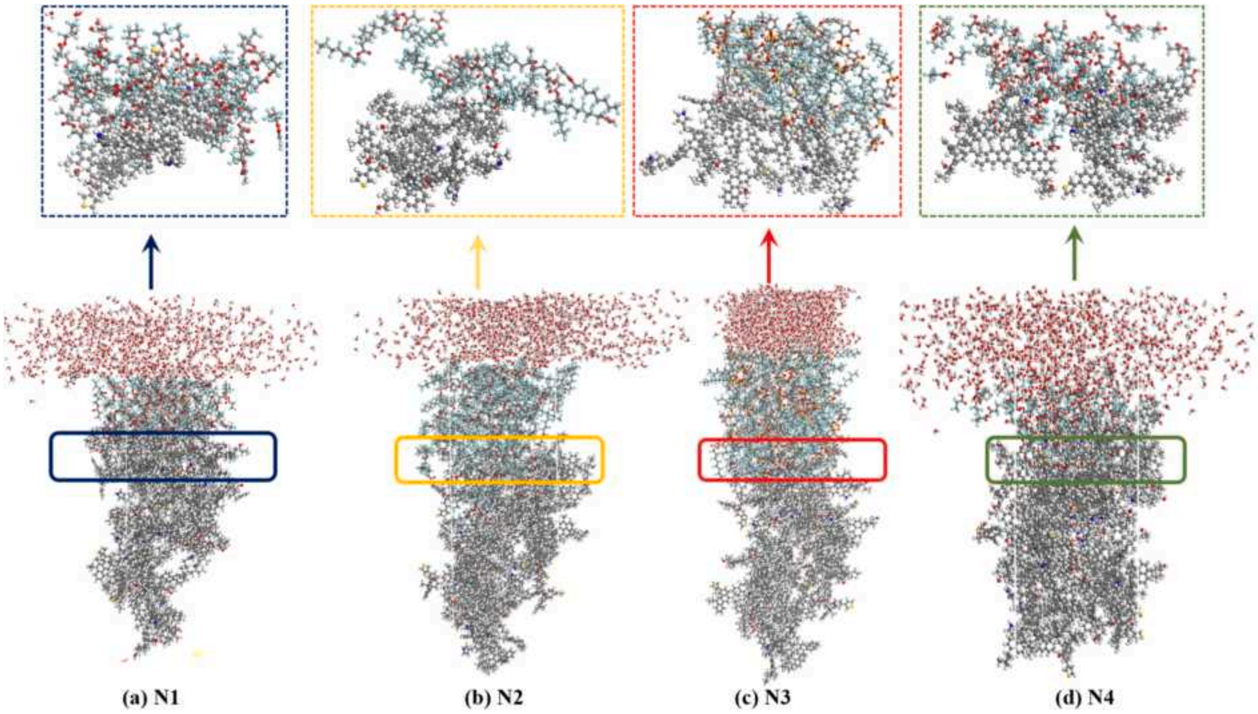

Fig. 11. The equilibrium configuration between fluoroalkane solution-water-coal.

fluorocarbon solution, which migrates the solution from the inside to the gas–liquid interface. In contrast, the hydrophobic fluorocarbon tail chain of PFA is relatively short. It may form a more stable interface layer between coal dust particles and the solution, prolonging the wetting time and impeding migration. Therefore, the ability of coal dust to enter the solution from the gas–liquid interface when adsorbed and enveloped by the fluorocarbon solution depends on their respective molecular structures (Figs. 1 and 3).

Different aromatic and oxygen-containing functional group structures and varying fluorocarbon carbon chain lengths exist in the four fluorocarbons. Specifically, PFTA and PPM have identical lengths of eight-tail fluorocarbon carbon chains, but PFTA contains a —COOH functional group, while PPM contains benzene rings, —OH, and $—SO_2$ functional groups. Compared to PPM, PFTA demonstrates a more pronounced settling velocity and lower surface tension. The —COOH functional group in PFTA can form hydrogen bonds with the coal dust surface, thus exhibiting higher wetting efficiency during the wetting process. Additionally, the fluorocarbon carbon chain lengths of PFA and PFPA are relatively short, being $—C_2F_5$ and $—C_3F_7$, respectively. However, PFPA, compared to PFA, has more hydrophilic head groups, with two additional $—CH_2$ groups. It results in PFPA outperforming PFA in immersion wetting performance, as it more readily forms hydrogen bonds with water, thereby more rapidly covering the coal dust surface and facilitating the wetting process. Conversely, the lower content of hydrophilic groups in PFA may require a longer time to contact and wet the coal dust surface effectively. Although the aromatic and oxygen-containing functional group structures of PFTA and PFPA are the same, their fluorocarbon carbon chain lengths are different, being $—C_8F_7$ and $—C_3F_7$, respectively. At solution concentrations below 0.1 %, PFTA performs better than PFPA in immersion and collision wetting. It may be because, at low concentrations, the longer fluorocarbon chain of PFTA is more conducive to forming a stable adsorption layer, reducing the surface tension of coal dust, thereby promoting the wetting process. With increasing concentration, as the similarity between the two solutions increases, the differences in their wetting performance gradually diminish.

Considering all the above analysis, the molecular structure of fluorocarbon solutions plays a crucial role in their performance in the solution. Longer fluorocarbon chains facilitate the formation of stable adsorption layers, enhancing the wetting ability on the surface of coal dust. However, due to its carboxyl group structure, PFA may exhibit superior immersion wetting performance at low concentrations. Therefore, the performance of various solutions varies at different concentrations. Immersion wetting performance: it demonstrates excellent immersion wetting performance at low concentrations, but at higher concentrations, it may slightly lag behind PFTA and PPM.

3.2. *Wetting mechanism analysis*

3.2.1. *Equilibrium configurations of different systems*

Fig. 11 illustrates the adsorption-wetting equilibrium configurations of four fluoroalkane solution/water/coal systems. As the wetting process occurs on the coal surface, the morphology of wetting adsorption of fluoroalkane solution on the coal surface undergoes a series of changes. The four fluoroalkane solutions exhibit lateral aggregation upon equilibrium, especially with PFPA and PFTA structures covering the coal surface. In this state, the hydrophobic fluoroalkane carbon chains are mainly concentrated on the side close to the coal surface. At the same time, the hydrophilic head groups, such as carboxyl groups, face toward the aqueous phase at the solid–liquid interface, aiding in reducing the surface tension of water and the interfacial tension at the solid–liquid interface. This change effectively increases the adsorption area, providing a broader contact range for the wetting process. Meanwhile, hydrophilic groups such as carboxyl groups in the PFPA solution adhere to the coal molecules, attracting water molecules to contact the coal surface and thus wetting the coal dust.

3.2.2. *The interaction energy of fluoroalkane solution on the coal surface*

In MD simulations, the variations in the wetting performance of fluoroalkane solutions on the coal surface can be quantified by the changes in the interaction strength among the system's fluoroalkane solution, coal, and water. The interaction energies between the fluoroalkane solutions and coal dust in four different systems are calculated using the formula (4) below.

Table 4
The interaction energy of four different fluorocarbon solution systems.

System	*Energy/(kcal/com)*							
	E_{int}	E_{total}	E_{water}	E_{coal}	E_{fs}	$E_{coal+water}$	$E_{coal+fs}$	$E_{water+fs}$
PFPA	−5757.25	−9826.01	3373.04	4302.87	−293.25	7675.91	3544.21	3079.79
PFTA	−4388.28	−5235.49	2556.41	4825.01	−767.85	7381.43	3635.23	1705.86
PPM	2850.18	9742.11	3222.68	8436.22	1551.30	11658.89	9709.94	4672.04
PFA	812.75	9943.52	2414.37	10384.43	−86.42	12790.29	9967.31	2388.60

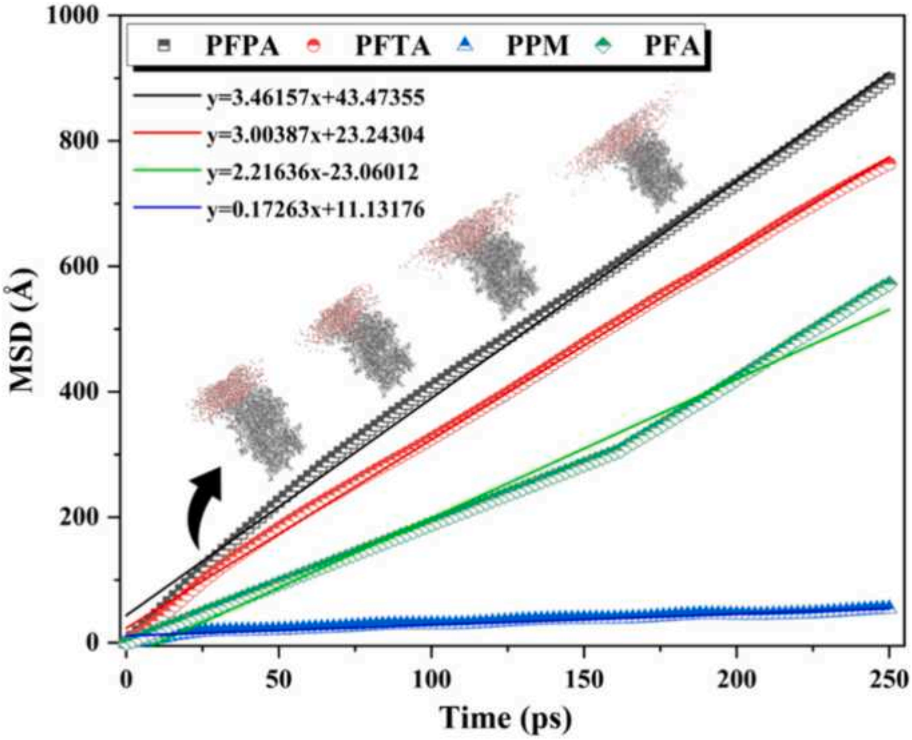

Fig. 12. MSD curves of water molecules around four different fluorocarbon solutions.

$$E_{\text{int}} = \left(E_{total} - E_{coal} - E_{coal+water} - E_{fs} + E_{fs+water} + E_{water} + E_{fs+coal}\right)/2 \quad (4)$$

In the Equation, E_{int} represents the interaction energy of the system, E_{total} represents the total energy of the entire adsorption system, E_{coal} represents the energy of the coal surface, E_{fs} represents the energy of the fluoroalkane solution, E_{water} represents the energy of water, $E_{coal+water}$ represents the total energy of water and coal, $E_{fs+coal}$ represents the total energy of the fluoroalkane solution and coal system, and $E_{fs+water}$ represents the total energy of the fluoroalkane solution and water system. The smaller the interaction energy E_{int} of the system, the stronger the wetting performance between the fluoroalkane solution and coal dust. It indicates a more stable wetting equilibrium and favorable adsorption of the fluoroalkane solution on the coal dust surface. The calculated interaction energies of the entire system are shown in Table 4, revealing that the stability follows the order PFPA > PFTA > PPM > PFA, indicating that the wetting abilities of the four surfactants on the coal dust surface are in the order PFPA > PFTA > PPM > PFA. Additionally, the interaction energies of the PFPA and PFTA systems are negative, indicating that the adsorption wetting process between these two fluoroalkane solutions and coal dust can occur spontaneously. It aligns with the results of the immersion wetting mentioned above.

3.2.3. Analysis of water molecule migration rate

The wetting behavior between fluoroalkane solution and coal dust affects the dynamics of water molecules. For molecules on the coal surface, MSD can display their diffusion degree and motion trajectory in space, thus assessing the diffusion characteristics of the molecules. By calculating the self-diffusion coefficient D, the diffusion speed of fluoroalkane solution molecules near the coal surface can be understood, inferring their wetting performance and behaviour [55]. The calculation formulas for MSD and D are shown in Eqs. (5) and (6).

$$MSD(t) = \frac{1}{N}\sum_{i=1}^{N}|r_i(t) - r_i(0)|^2 \quad (5)$$

$$D = \lim_{t\to\infty}\frac{MSD(t)}{6t} \quad (6)$$

In the Equation, N represents the number of water molecules, and $r_i(t)$, $r_i(0)$ denotes the molecule's position vectors at time t = i and t = 0.

Fig. 12 shows the MSD curves of water molecules around coal in four different fluorocarbon solutions. Linear fits are applied to the MSD curves. The obtained diffusion coefficients (D values) for water molecules in the four systems are as follows: $D_{PFPA} = 0.577$ Å/ps, $D_{PFTA} = 0.501$ Å/ps, $D_{PFA} = 0.369$ Å/ps, and $D_{PPM} = 0.029$ Å/ps. It indicates that the migration rates of water molecules in the PFPA and PFTA systems are increased, intensifying their movement and enhancing the interaction between coal surfaces and water, thus promoting the wetting process of coal dust. This wetting performance order aligns with the wetting analysis.

3.2.4. Relative concentration analysis

Fig. 13 shows the relative concentration distribution along the Z-axis

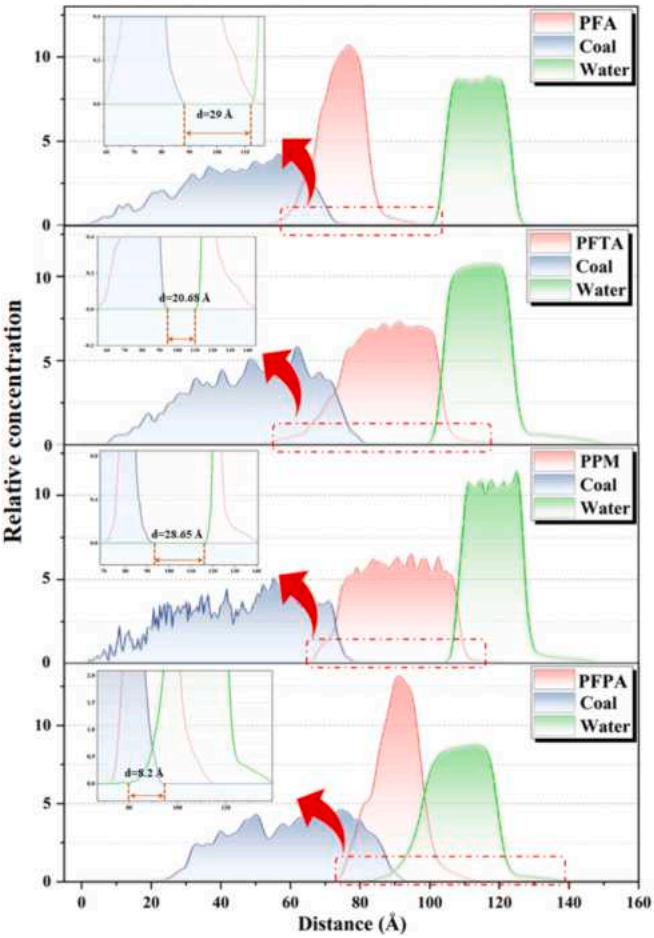

Fig. 13. The relative concentration distribution of different fluorocarbon solution systems.

of different components in the equilibrium state of the simulated systems for the four fluorocarbon solutions. The relative concentration ranges for PFPA, PFTA, PPM, and PFA are 70.04–115.06 Å, 58.99–136.24 Å, 73.44–134.92 Å, and 60.17–109.36 Å, respectively. From the enlarged area of PFPA in Fig. 13, after 250 ps of simulation, longitudinal diffusion of water molecules within the system is observed. The width of the overlap between water molecules and PFPA solution reaches 8.2 Å, indicating that compared to other solutions, PFPA solution exhibits stronger water absorption and wetting properties, allowing some water molecules to penetrate the fluorocarbon solution and adsorb onto the coal dust surface.

4. Conclusions

The wetting mechanisms of four distinct fluorocarbon solutions and their interactions with coal dust surfaces are investigated via experimental and MD simulation approaches. The main conclusions are as follows.

(1) Analysis of surface tension properties indicates that, at concentrations exceeding 0.1 %, the ability of solutions to reduce surface tension follows the order PFA > PFTA > PFPA > PPM. This trend is primarily attributed to the impact of fluorocarbon carbon chains on the adsorption configuration of solutions at the gas–liquid interface, facilitating a rapid reduction of coal dust surface tension at lower concentrations.

(2) Various organic functional group structures on coal dust surfaces markedly affect the wetting of solutions. Comparative analysis reveals enhanced adsorption on coal dust surfaces following treatment with fluorocarbon solutions, as evidenced by prominent C—O and —CH2 peaks. Specifically, the adsorption pattern of C—O structures follows PFPA > PFPA ≈ PFA > PPM, indicating the propensity of fluorocarbon solutions containing C—O structures to adsorb on coal dust surfaces, thus facilitating wetting. MD simulations corroborate these findings, which are consistent with FTIR experimental results, with interaction energy and water molecule migration rates indicating increased adsorption and accelerated wetting for PFPA and PFTA.

(3) Immersion wetting is identified as more discernible than collision contact wetting and adsorption wetting in assessing the wetting performance of fluorocarbon solutions on coal dust. Below 0.1 % concentrations, PFPA and PFTA exhibit immersion times of less than 5 min, significantly shorter than those of PFA and PPM solutions, underscoring their superior low-concentration immersion wetting capabilities. It can be attributed to the hydrophilicity of carboxyl groups in PFPA and PFTA, expediting wetting and permeation of water molecules on coal dust surfaces. Analysis of collision and adsorption wetting results reveals PFPA's superior performance over PFTA, attributed to its longer fluorocarbon chain length. Consequently, the comprehensive wetting capabilities of the four fluorocarbon solutions rank as follows: PFPA > PFTA > PFA > PPM.

(4) Equilibrium configurations of fluorocarbon solutions demonstrate stable configurations characterized by the insertion of hydrophilic polar groups into the aqueous phase, while hydrophobic fluorocarbon tail chains adsorb onto coal surfaces. It suggests that surfactant molecules enhance coal surface wetting through bridging effects. Interaction energy, surfactant molecule distribution along the Z-axis, and water molecule diffusion rates follow the sequence PFPA > PFTA > PFA > PPM, corroborating their wetting properties. These findings align with wetting performance analyses.

CRediT authorship contribution statement

Kai Wang: Writing – review & editing, Methodology, Conceptualization. **Min Xu:** Writing – original draft, Software, Investigation. **Biao Zhou:** Methodology, Investigation. **Dezheng Wang:** Software, Investigation. **Kaijie Chen:** Investigation.

Declaration of competing interest

The authors declare that they have no known competing financial interests or personal relationships that could have appeared to influence the work reported in this paper.

Data availability

Data will be made available on request.

Acknowledgments

This work was supported by the Beijing Nova Program (No. Z211100002121102, No. 20220484236), the Beijing Municipal Natural Science Foundation (No. 8222029), the National Fire and Rescue Bureau Science and Technology Plan Project (No. 2023XFCX21), Liuzhou Science and Technology Plan Project (No. 2023JRZ0102), The Tianjin Science and Technology Plan Project (No. 22JCZDJC00880, No. 22JCZDJC00900), the Ministry of Education Chunhui Plan Collaborative Research Project (No. HZKY202200132), the National Foreign Experts Program (No. G2023123004L), and the Key Laboratory of Fire Protection Technology for Industry and Public Building Ministry of Emergency Management (No. 2023KLIB02).

References

[1] W. Mingyue, H. Xiangming, Z. Qian, L. Wei, Z. Yanyun, H. Zhenglong, Study on preparation and properties of environmentally-friendly dust suppressant with semi-interpenetrating network structure, J. Clean. Prod. 259 (2020) 120870.

[2] Y. Wei, J. Li, J. Wang, Respirable dust detection and optimization of dust prevention measures in fully mechanized face of coal mine, in: IOP Conference Series: Earth and Environmental Science, vol. 330, 2019, p. 032012.

[3] W. Xiaonan, Study on Synergistic Effect of Surfactant Compound on Coal Dust Wettability [Doctor], Anhui University of Science & Technology, 2020.

[4] G. Zhou, Y. Ma, T. Fan, G. Wang, Preparation and characteristics of a multifunctional dust suppressant with agglomeration and wettability performance used in coal mine, Chem. Eng. Res. Des. 132 (2018) 729–742.

[5] L. Chanthaphasouk, K. Maneeintr, P. Meechumna, S. Luengwattanapong, C. Poonjarernsilp, Evaluation of the risk factors on coal dust explosion in warehouse, in: MATEC Web of Conferences, vol. 77, 2016, p. 06014.

[6] Y. Jiang, P.J. Zong, B. Tian, F.F. Xu, Y.Y. Tian, Y.Y. Qiao, et al., Pyrolysis behaviors and product distribution of Shenmu coal at high heating rate: a study using TG-FTIR and Py-GC/MS, Energ. Conver. Manage. 179 (2019) 72–80.

[7] H. Song, G. Liu, J. Zhang, J. Wu, Pyrolysis characteristics and kinetics of low rank coals by TG-FTIR method, Fuel Process. Technol. 156 (2017) 454–460.

[8] H. Zhang, W. Nie, J. Yan, Q. Bao, H. Wang, H. Jin, et al., Preparation and performance study of a novel polymeric spraying dust suppression agent with enhanced wetting and coagulation properties for coal mine, Powder Technol. 364 (2020) 901–914.

[9] G. Zhou, B. Feng, W. Yin, J. Wang, Numerical simulations on airflow-dust diffusion rules with the use of coal cutter dust removal fans and related engineering applications in a fully-mechanized coal mining face, Powder Technol. 339 (2018) 354–367.

[10] Z. Zhao, Y. Zhao, X. Hu, W. Cheng, J. Hou, C. Song, Preparation and performance analysis of enteromorpha-based environmentally friendly dust suppressant, Powder Technol. 393 (2021) 323–332.

[11] P. Chang, Z. Zhao, G. Xu, A. Ghosh, J. Huang, T. Yang, Evaluation of the coal dust suppression efficiency of different surfactants: a factorial experiment, Colloids Surf. A Physicochem. Eng. Asp. 595 (2020) 124686.

[12] H. Zhang, W. Nie, Y. Liu, H. Wang, H. Jin, Q. Bao, Synthesis and performance measurement of environment-friendly solidified dust suppressant for open pit coalmine, J. Appl. Polym. Sci. 135 (29) (2018) 46505.

[13] V.A. Arkhipov, D.Y. Paleev, Y.F. Patrakov, A.S. Usanina, Coal dust wettability estimation, J. Min. Sci. 50 (3) (2014) 587–594.

[14] Q. Bao, W. Nie, C. Liu, H. Zhang, H. Wang, H. Jin, et al., The preparation of a novel hydrogel based on crosslinked polymers for suppressing coal dusts, J. Clean. Prod. 249 (2020) 119343.

[15] F.Q. Cheng, S.Y. Cheng, Y.X. Guo, L.Q. Cao, Synthesis of coal dust depressor and its application in preventing coal dust, Adv. Mat. Res. 482–484 (2012) 2301–2306.

[16] C. Xu, D. Wang, H. Wang, H. Xin, L. Ma, X. Zhu, et al., Effects of chemical properties of coal dust on its wettability, Powder Technol. 318 (2017) 33–39.

[17] Q. Zhou, B. Qin, Coal dust suppression based on water mediums: a review of technologies, Fuel 302 (2021) 121196.

[18] Z. Lu, Z. Lei, M.N. Zafar, Synthesis and performance characterization of an efficient environmental-friendly Sapindus mukorossi saponins based hybrid coal dust suppressant, J. Clean. Prod. 306 (2021) 127261.

[19] Q. Wei, Y. Zhang, K. Chen, B. Liu, X. Meng, X. Zhang, et al., Preparation and performance of novel APP/NaY–Fe suppressant for coal dust explosion, J. Loss Prev. Process Ind. 69 (2021) 104374.

[20] Y. Liu, W. Nie, H. Jin, H. Ma, Y. Hua, P. Cai, et al., Solidifying dust suppressant based on modified chitosan and experimental study on its dust suppression performance, Adsorpt. Sci. Technol. 36 (1–2) (2017) 640–654.

[21] Q. Liao, G. Feng, Y. Fan, S. Hu, H. Shao, Y. Huang, Experimental investigations and field applications of chemical suppressants for dust control in coal mines, Adv. Mater. Sci. Eng. 2018 (2018) 1–9.

[22] G.H. Ni, Q. Sun, M. Xun, H. Wang, Y.H. Xu, W.M. Cheng, et al., Effect of NaCl-SDS compound solution on the wettability and functional groups of coal, Fuel 257 (2019) 116077.

[23] Q. Zhang, G. Zhou, Y. Hu, W. Wang, Experimental investigation on wetting mechanism for coal dust with different metamorphic degree based on infrared spectrum and 13C-NMR, Surf. Interface Anal. 52 (8) (2020) 470–485.

[24] Q. Zhou, B. Qin, H. Huang, Research on the formation mechanism of magnetized water used to wet coal dust based on experiment and simulation investigation on its molecular structures, Powder Technol. 391 (2021) 69–76.

[25] X. Chen, T. Ma, X. Zhai, C. Lei, Thermogravimetric and infrared spectroscopic study of bituminous coal spontaneous combustion to analyze combustion reaction kinetics, Thermochim. Acta 676 (2019) 84–93.

[26] Z. Wei, L. Baiquan, L. Tong, Construction of Pingdingshan coal molecular model based on FT-IR and 13C-NMR, J. Mol. Struct. 1262 (2022) 132992.

[27] Q. Lu, S. Qin, W. Wang, K. Gao, J. Xing, Geochemistry of Late Permian coals from the Moxinpo mine, Chongqing, Southwestern China: emphasis on petrology, minerals, and organic matter, Appl. Geochem. 149 (2023) 105558.

[28] M. Xu, L. Xin, W. Liu, X. Hu, W. Cheng, C. Li, et al., Study on the physical properties of coal pyrolysis in underground coal gasification channel, Powder Technol. 376 (2020) 573–592.

[29] C. Liping, Study on the Formation and Release of Nitrogen-containing Compounds during Coal Pyrolysis and Gasification [Doctor], Taiyuan University of Technology, 2004.

[30] X. Ding, D. Wang, Z. Luo, T. Wang, J. Deng, Multi-scale study on the agglomerating and wetting behaviour of binary electrolyte-surfactant coal dust suppression based on multiple light scattering, Fuel 311 (2022) 122515.

[31] M. Zhang, Y.-Y. Zhao, X.-M. Hu, Y. Feng, W.-M. Cheng, W.-H. Liu, et al., Study on the adsorption and dust suppression mechanism of urease-producing bacteria on coal dust, Powder Technol. 409 (2022).

[32] X. Ding, T. Ma, W. Zhao, Z. Luo, T. Wang, Y. Sheng, et al., Airborne high oil-content coal particles suppression via the electrolyte accelerated application of hydrocarbon and short-chain fluorocarbon surfactants, Fuel 332 (2023).

[33] X. Ding, D. Wang, Z. Luo, G. Xu, T. Wang, F. Cheng, Investigation of agglomerating and wetting behaviour during coal dust suppression via the synergistic application of hydrocarbon and short-chain-fluorocarbon surfactants in the presence of electrolytes, Powder Technol. 404 (2022).

[34] F.Y. Dai, H.Y. Hu, A.H. Zhang, Suitability study on fractal model of organic shale pore, Coal Sci. Technol. 47 (2) (2019) 168–175.

[35] W. Niu, W. Nie, Q. Bao, Q. Tian, F. Liu, R. Li, et al., Interactions between fluorocarbon surfactant and coal dust at macro, meso and molecular scales and their applications in coal dust control, Chem. Eng. J. 475 (2023).

[36] Y. Jing, T. Yunzhen, W. Zhenhua, S. Yandong, Z. Wenbin, Study on the coal dust surface characteristics and wetting mechanisn, J. China Coal Soc. 07 (2007) 737–740.

[37] J. Yang, Study on Wetting Mechanism of Coal Dust [Doctor], Shandong University of Science and Technology, 2008.

[38] W. Xiukun, Research and Application of Physical and Chemical Characteristics of Respiratory Coal Dust, Shandong University of Science and Technology, [Master], 2010.

[39] J. Feng, J. Li, W. Li, Influences of chemical structure and physical properties of coal macerals on coal liquefaction by quantum chemistry calculation, Fuel Process. Technol. 109 (2013) 19–26.

[40] M. Yuan, W. Nie, H. Yu, J. Yan, Q. Bao, W. Zhou, et al., Experimental and molecular dynamics simulation study of the effect of different surfactants on the wettability of low-rank coal, J. Environ. Chem. Eng. 9 (5) (2021) 105986.

[41] H. Jin, Y. Zhang, H. Dong, Y. Zhang, Y. Sun, J. Shi, et al., Molecular dynamics simulations and experimental study of the effects of an ionic surfactant on the wettability of low-rank coal, Fuel 320 (2022) 123951.

[42] W. Nie, M. Yuan, Q. Bao, J. Yan, W. Zhou, C. Guo, et al., Experimental and molecular dynamics simulation research on compound dust suppressant based on locust bean gum, Adv. Powder Technol. 33 (3) (2022) 103485.

[43] F. Xu, S. Pan, C. Liu, D. Zhao, H. Liu, Q. Wang, et al., Construction and evaluation of chemical structure model of Huolinhe lignite using molecular modeling, RSC Adv. 7 (66) (2017) 41512–41519.

[44] H.-Y. Lu, X.-F. Li, C.-Q. Zhang, J.-Y. Chen, L.-G. Ma, W.-H. Li, et al., Experiments and molecular dynamics simulations on the adsorption of naphthalenesulfonic formaldehyde condensates at the coal-water interface, Fuel 264 (2020) 116838.

[45] Z. Dong, S. Liu, X. Nie, Y. Zhang, K. Dong, J. Wang, Experimental and molecular simulation research on the effect of metal ions on the stability of SDS foam, Energy Fuel 36 (1) (2021) 521–526.

[46] J. Sun, G. Zhou, D. Gao, Z. Wei, N. Wang, Preparation and performance characterization of a composite dust suppressant for preventing secondary dust in underground mine roadways, Chem. Eng. Res. Des. 156 (2020) 195–208.

[47] M. Yuan, W. Nie, W. Zhou, J. Yan, Q. Bao, C. Guo, et al., Determining the effect of the non-ionic surfactant AEO9 on lignite adsorption and wetting via molecular dynamics (MD) simulation and experiment comparisons, Fuel 278 (2020) 118339.

[48] J. Meng, L. Wang, S. Zhang, Y. Lyu, J. Xia, Effect of anionic/nonionic surfactants on the wettability of coal surface, Chem. Phys. Lett. 785 (2021) 139130.

[49] J. Gan, D. Wang, Z. Xiao, Y.-n. Wang, K. Zhang, X. Zhu, et al., Experimental and molecular dynamics investigations of the effects of ionic surfactants on the wettability of low-rank coal, Energy 271 (2023) 127012.

[50] J. Wang, Z. Wei, Y. Liu, X. Jing, F. Liu, H. Cao, et al., Preparation and molecular simulation of an environmentally friendly dust-fixing agent based on chitosan-gelatin, Environ. Sci. Pollut. Res. Int. 30 (42) (2023) 95312–95325.

[51] J. Zhao, S. Tian, P. Li, H. Xie, J. Cai, Molecular dynamics simulation and experimental research on the influence of SiO_2-H_2O nanofluids on wettability of low-rank coal, Colloids Surf. A Physicochem. Eng. Asp. 679 (2023) 132580.

[52] D. Wang, Q. Zeng, Study on the inhibitory effect of inhibitor based on the coal molecular structure analysis: a case study of Zhundong coal, Xinjiang, China, J. Mol. Struct. 1301 (2024) 137446.

[53] X. Wang, Study on Synergistic Effect of Surfactant Combination on Wettability of Coal Dust [Ph. D], Anhui University of Science and Technology, 2020.

[54] T. Young, An essay on the cohesion of fluids, Proc. R. Soc. Lond. 95 (1805) 65–87.

[55] Z. Liu, G. Zhou, J. Duan, D. Liu, Q. Zhang, S. Guo, Preparation of composite high-efficiency dust suppressant and relevant molecular dynamics simulation for wetting coal surface, Fuel 296 (2021) 120579.